

Non-destructive Determination of Chlorophyll Concentration in the Leaves, Sepals and Bracts of *Hibiscus rosa-sinensis* and Leaves of *Chrysanthemum* × *morifolium*

Kit D. Jernshøj^{1*} • Søren Hassing¹ • Carl-Otto Ottosen²

¹ Institute of Sensors, Signals and Electrotechnics (SENSE), University of Southern Denmark, Campusvej 55, 5230 Odense M, Denmark

² Department of Horticulture, Aarhus University, Kirstinebjergvej 10, 5792 Årslev, Denmark

Corresponding author: * kdj@sense.sdu.dk

ABSTRACT

An analysis of the composition and concentration of pigments – both chlorophyll (Chl) and other protective pigments, is often critical, when analyzing the reaction of plants to the effects of abiotic conditions. Therefore, a rapid non-destructive method for determining pigment concentrations accurately would be an advantage. The chlorophyll (Chl) concentrations in the leaves, sepals and bracts from *Hibiscus rosa-sinensis* and the leaves from *Chrysanthemum* × *morifolium* were determined *in vivo* by applying two different algorithms to the reflectance and transmittance data obtained from a spectrophotometer with an integrating sphere. As sepals and bracts from *Hibiscus* are small, a modification was needed using a mask. When measuring reflectance, a mask has been combined with a properly focused sample beam, to avoid direct illumination of the mask. The transmittance spectra are achieved by a combination of a lens setup and an attachment of the sample to the entrance port. Two different models have been used for the calculation of Chlorophyll concentration. The first model is based on an empirical relationship between reciprocal reflectance and Chl concentration, whereas the second model is based on the optical characteristics of the leaf. Our aim with the experiments was to improve the methods for non-invasive detection of Chl in ornamental plant species and leaf types.

Keywords: reflectance, transmittance, secondary metabolites

Abbreviations: Chl, chlorophyll; NIR, near-infrared

INTRODUCTION

The possibility of estimating the Chlorophyll (Chl) concentration non-destructively is an attractive alternative to the cumbersome process of chemical extraction (Arnon 1949). Being able to determine a pigment concentration quickly *in vivo* provides access to the content of secondary pigments such as carotenoids or anthocyanins, which moreover can provide valuable information about the physiological status of a plant in relation to light stress (Smillie and Hetherington 1999; Gitelson *et al.* 2009). Nutrient deficiencies will also be reflected in the pigment composition of a leaf, especially with respect to nitrogen (Fritsch and Ray 2007). As an example, an anthocyanin reflectance index, with reflectances in the green and red edge spectral bands (525 to 555 nm and 695 to 735 nm) and a modified anthocyanin reflectance index, employing in addition the near-infrared (NIR) band, have been used to accurately estimate leaf anthocyanin (Gitelson *et al.* 2009).

Two principally different kind of methods based on either reflectance or transmittance data (Gitelson *et al.* 2003; Gitelson and Merzlyak 2004) or on reflectance and transmittance data (Yamada and Fujimura 1991) can be used to evaluate the pigment concentrations in leaves non-destructively. The first kind of method is based on only the reflectance or transmittance values obtained at selected wavelengths and an empirical relationship between the reflectance or transmittance and the Chl concentration. This kind of method will be termed the R/T-EMP method. In the algorithms of the simplest R/T-EMP method, the Chl concentration is approximately proportional to the ratio of two reflectance values obtained at two selected wavelengths (or transmittance values), where the choice of wavelength de-

pends on the plant species (Carter and Knapp 2001; Carter and Spiering 2002). The R/T-EMP method can moreover be made applicable to a larger number of different plant species by basing the choice of the distinct wavelengths on a larger statistical plant material and by developing the algorithms further by incorporating the reflectance or transmittance values from more wavelengths (Gitelson *et al.* 2003; Gitelson and Merzlyak 2004; Gitelson *et al.* 2009). Commercial equipment used for estimating the Chl concentrations of plants in the field are based on the R/T-EMP method, e.g. FieldScout CM 1000 (FieldScout CM 1000 Chlorophyll Meter, Operation Manual 2009) and SPAD (SPAD 502 Plus Chlorophyll Meter Product Manual 2009).

The second kind of method is based on selected reflectance and transmittance values combined with a theoretical modeling and knowledge of the optical characteristics of a leaf. This method will be termed the RT-MOD method.

The aim of the present paper is threefold: a) To accurately and reproducibly determine the pigment concentration in absorbing and scattering samples of varying size, such as the sepals, bracts and leaves from *Hibiscus* based on reflectance and transmittance data obtained on a research spectrophotometer equipped with an integrating sphere; b) To address the pitfalls existing, when determining the Chl concentration in small samples of plant material by measuring the reflectance and transmittance with an integrating sphere; c) To compare the calculations of the Chl concentration in the sepals, bracts and leaves from *Hibiscus* performed with the R/T-EMP and RT-MOD methods based on the accurate reflectance and transmittance data.

The optimized measurements of reflectance and transmittance, which enables an accurate calculation of the Chl concentration, performed on the research spectrophotometer

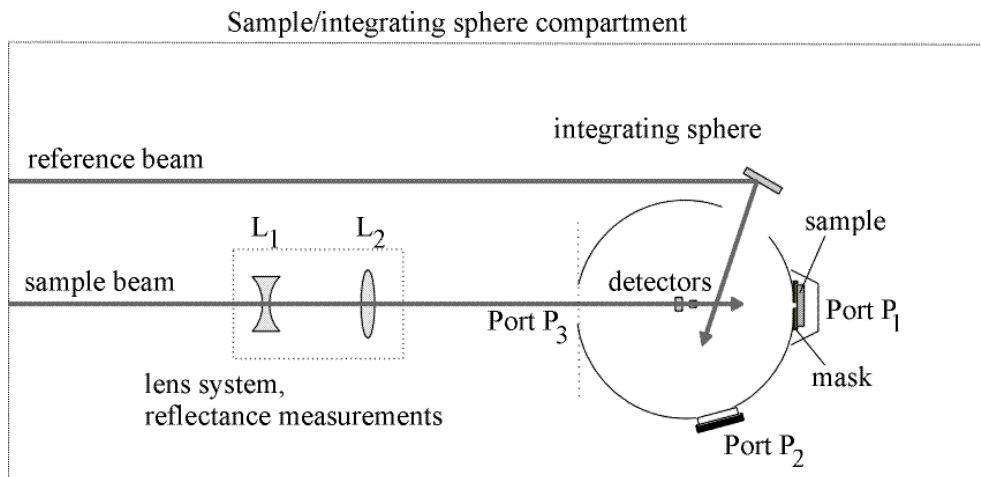


Fig. 1 A schematic drawing of the integrating sphere, which is placed in the sample compartment of the spectrophotometer. Besides, are shown the introduction of a lens setup in the sample beam and the mask and sample in the sample port P_1 , which is applicable for reflectance measurements. The lens system consists of lenses L_1 and L_2 , the focal length of these are -50 mm and 100 mm, the distance between these is 106 mm and the distance between the lens L_2 and the port P_3 of the integrating sphere is 10 cm.

combined with an integrating sphere may serve the purpose as reference concentration instead of the results obtained by chemical extraction (Arnon 1949).

The R/T-EMP method considered in this paper is based on an algorithm (Gitelson and Merzlyak 2004; Gitelson *et al.* 2009), while the RT-MOD method is originally developed by (Yamada and Fujimura 1991) for determination of the Chl concentration in dicotyledonous leaves. We have in the study included different leaf types from a *Hibiscus rosa-sinensis*, i.e. sepals, bracts and leaves from *Chrysanthemum x morifolium* with varying size and tissue composition and different expected concentrations of Chl and carotenoids. In spectroscopy, transmittance is the fraction of incident light at a specified wavelength that passes through a sample (either a solution or in this case an object (a leaf)), while reflectance is an expression of the ratio of the total amount of radiation, as of light, reflected by a (leaf) surface to the total amount of radiation incident on the (leaf) surface and both these values are included in the models used. The reflectance and transmittance data must be obtained by using the most optimal setup with respect to accuracy and reproducibility (Jernshøj and Hassing 2009).

MATERIALS AND METHODS

Measurements

The spectrophotometer used to perform the measurements is a stationary double beam spectrophotometer (Perkin Elmer, Lambda 900) with a Labsphere integrating sphere option (LabSphere PELA 1000). The integrating sphere, which is 150 mm in diameter, is equipped with 25 mm circular port apertures, for reflectance and transmittance measurements, respectively. This means that samples smaller than the port apertures necessitates a modification of the experimental setup. The spectrophotometer covers the wavelength range 185-3300 nm. In the ultraviolet and visible range the signal is detected by a photomultiplier and in the near infrared range by a lead sulfide detector (PbS). The use of an integrating sphere ensures diffuse illumination of the sample and collection of diffuse reflected or transmitted light.

A schematic drawing of the principles behind the reflectance measurements is shown in **Fig. 1** and behind the transmittance measurements in **Fig. 3**. The spectrophotometer is a scanning instrument, which measures the diffuse reflectance as well as the transmittance of a sample versus wavelength, $R(\lambda)$ and $T(\lambda)$. The procedure of the reflectance measurement is as follows: the sample is placed in the port P_1 of the sphere and the light intensity backscattered by the sample into the solid angle 2π is collected by the sphere and captured by the detector. The ratio between this intensity and the intensity scattered from a reference standard

placed in the port P_2 is monitored at every wavelength in the chosen region. Before the measurement the instrument must be calibrated by measuring the same ratio with the exception that the sample in port P_1 is replaced with the standard. The reflectance of the sample $R(\lambda)$ is then given as the ratio between the result of the measurement performed on the sample and the calibration measurement. The principle of the transmittance measurement $T(\lambda)$ is the same as for the reflectance measurements, except that the sample is placed in the port P_3 and the reference is in this case air. Further details can be found in the integrating sphere manual (LabSphere PELA 1000), and in the Jernshøj and Hassing (2009) reference.

Plants were obtained from a commercial nursery in salable size and had been grown according to normal practice and fully fertilized so leaves could be picked at random for measurements. *Hibiscus rosa-sinensis* 'Cairo' (Malvaceae) and *Chrysanthemum x morifolium* Ramat 'Yoauburn' (Asteraceae) were used as they represent a high light plant species and an adaptive species. One of the primary goals was to obtain reflectance and transmittance spectra of the bracts and sepals of *Hibiscus*. These are too small to fit the apertures of the sphere, while *Chrysanthemum* leaves are of sufficient size. The plant parts were removed from the plants just before measurement and placed at entrance port P_3 or at the sample port P_1 . Since the plant material was fresh and each measurement took place over a very short period, the effect of the amount of secondary metabolites should not be of importance as no degradation took place. Leaves could have remained on the plants making the measurements both non-destructive and non-invasive, but for flower parts the measurements were only non-invasive.

Since the size of the bracts and sepals of *Hibiscus* are smaller than the apertures of the sphere (i.e. the ports P_1 and P_3) and since the beam provided by the spectrophotometer has a larger cross sectional area than the size of these samples, some modifications have to be made. The simplest of these modifications is to use a mask to hold the samples in place, thereby reducing the aperture of the ports (Perkin Elmer, Lambda 900; LabSphere PELA 1000). The mask used in the reflectance measurements performed in this paper is made of 0.19 mm thick brass foil, which is painted a mat black and the aperture of the mask is chosen, so that the smaller of the samples just fills the aperture (**Fig. 2**). The aperture is therefore rectangular with the dimensions $2 \times 6 \text{ mm}^2$. Due to the large cross sectional area of the sample beam, the mask is directly illuminated, which as shown in reference (Jernshøj and Hassing 2009) leads to the first pitfall, namely wavelength- and sample-dependent scattering phenomena. These phenomena result in very large measuring errors, which depend on the structure and the optical properties of the sample. It is therefore not possible to find a both universal and accurate way to correct the reflectance data, which leads to an inaccurate calculation of the Chl concentration. To obtain the most accurate reflectance values of the small samples,

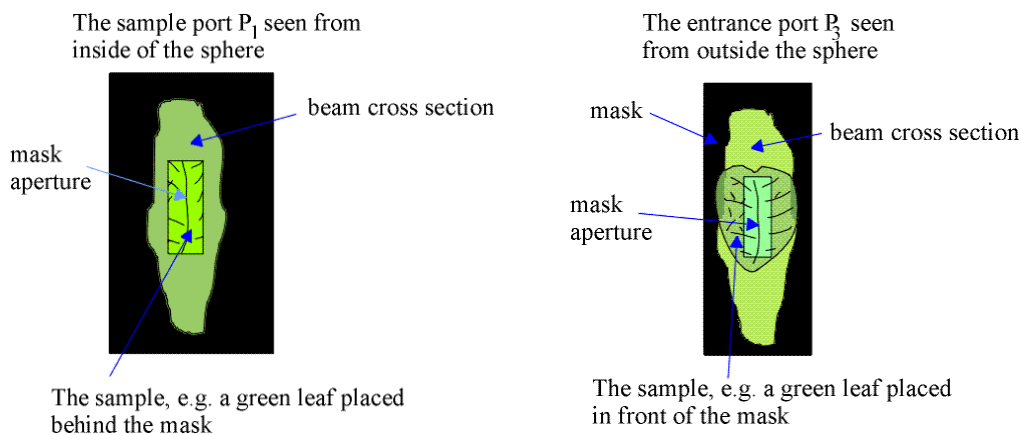


Fig. 2 The first subfigure in this figure shows a leaf and the mask placed in the sample port P_1 (reflectance measurements). The schematic drawing is made in order to illustrate the illumination of the mask, which also takes place during the transmittance measurements in port P_3 as shown in the other subfigure.

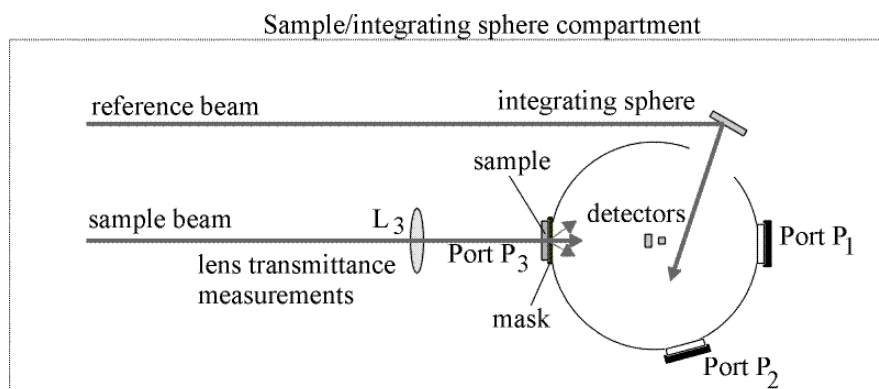


Fig. 3 A schematic drawing of the integrating sphere, which is placed in the sample compartment of the spectrophotometer. Besides are shown the introduction of a lens, L_3 , in the sample beam and the mask/suspension of the sample in the entrance port P_3 , which is applicable for transmittance measurements. The focal length of the lens L_3 is 50 mm and the distance to the integrating sphere is 4 cm.

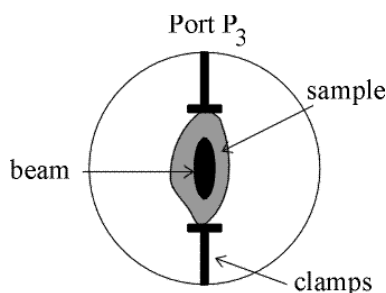


Fig. 4 A schematic illustration of how the sample has been suspended in the entrance port P_3 of the sphere during the transmittance measurements. The suspension consists of two clamps, which secures the sample and makes the use of a mask superfluous.

the measurements should satisfy the following requirements. First of all any illumination of the mask must be avoided. This is ensured by inserting focusing optics in the sample path as shown in **Fig. 1** combined with a careful adjustment of the mask. Secondly, the ratio between the mask aperture (which has been defined by the bracts) and the beam area should be chosen as large as possible. The data for the removable lens system, designed for the reflectance measurements performed in the present paper, is given in the caption of **Fig. 1**. The size of the focused beam in the reflection sample port P_1 with the lens system inserted is approximately $1 \times 4 \text{ mm}^2$.

Considering the transmittance measurements on small samples, it was found in (Jernshøj and Hassing 2009) that the accuracy of these is in general much higher than that of reflectance measurements. This may be ascribed to the nature of the transmittance measurements, where the low transmittance of the mask ensures

that only a small amount of the light illuminating the mask will enter the integrating sphere directly. Despite this, the most optimal way to obtain accurate transmittance spectra was concluded to be a combination of a focusing lens and an attachment of the sample to the entrance port P_3 . The attachment, which is shown in **Fig. 4**, is done by means of two thin ($3 \times 1 \text{ mm}$) rigid non-illuminated clamps. This measuring setup renders the use of the mask unnecessary, since the sample is freely suspended in the entrance port. The data of the removable lens is mentioned in the caption of **Fig. 3**. The size of the focused beam in the port P_3 with the lens inserted in the beam path is approximately $0.5 \times 4 \text{ mm}^2$.

Molecular and phenomenological absorption and scattering coefficients, Kubelka-Munck theory

The free molecules of plant pigments such as Chl, carotenoids and anthocyanins have characteristic absorption (UV/Visible, IR and NIR) and Raman spectra, which may be used to obtain information about the structure and chemical properties of these molecules. The spectra are typically measured on diluted solutions of the pigment molecules, where it is reasonable to assume that the molecules interact independently with the light with the result that the absorption and the scattering from the solution is proportional to the molar concentration of the pigment molecules. This is the basis for the Lambert-Beer law. In molecular spectroscopy performed on diluted solutions it is convenient to describe the absorption and scattering processes by an absorption cross section σ_{abs} and a scattering cross section σ_{scat} . σ_{abs} and σ_{scat} have the unit [area] and each of them defines an effective area of each pigment molecule as seen by the incoming beam of photons interacting with the molecule. Thus σ_{abs} and σ_{scat} are measures of the probability that a molecule either absorbs or scatters a photon with a particular wavelength and polarization. Theoretically the absorption and scattering cross sections may be expressed in terms of fundamental molecular

parameters through the application of quantum mechanics and a theoretical modeling of the molecules.

In the case of absorption measurements on a diluted solution of pigment molecules the absorption cross section is related to the macroscopic absorption coefficient associated with a volume element of the solution, α_{abs} in a simple manner following from the derivation of the Lambert-Beer law, $\sigma_{abs} = 10^3 (N_A C)^{-1} \alpha_{abs}$, where N_A is Avogadro's constant and C is the molar concentration of the absorbing pigment.

However, when the pigments are in their natural environment in the leaves or in other parts of the plant, the relations between σ_{abs} and σ_{scat} and the macroscopic counterparts, α_{abs} and α_{scat} will be much more complex due to the interactions among the pigment-molecules (e.g. formation of aggregates) and interactions between the pigment molecules and the molecules forming the matrix of the host material. The modeling of these interactions and how they should be incorporated in the theory of absorption and scattering processes requires a detailed knowledge of the system under investigation. This complexity is partially circumvented in the Kubelka-Munk (KM) theory (Kortüm 1969).

The KM theory is a phenomenological, two-flux theory which describes the transfer of radiation in a semi-homogeneous (or turbid) material consisting of light-scattering and light-absorbing particles imbedded in a homogeneous background material. The basic KM theory assumes diffuse illumination of the material, isotropic scattering distribution, infinite penetration depth, that scattering dominates over absorption and that the absorption is independent of the scattering. The two first conditions are met by using an integrating sphere when measuring reflectance (Kortüm 1969).

Several extensions of the original KM theory have been made, to cover also collimated illumination (Murphy 2006) and that the absorption may be a function of the scattering (Yang and Miklavcic 2005). The main advantage of the original KM theory is that it provides a simple relation between phenomenological absorption and scattering coefficients and the available experimental parameters, the diffuse reflectance and transmittance. The theory has in many cases of practical interest proven to be of sufficient accuracy, i.e. it is widely applied within areas such as color printing industry, textile and paint fabrication and in biological and medical physics.

The geometry in the KM theory is illustrated in Fig. 5. The figure shows a layer of a freely suspended turbid medium, which is diffusely illuminated. The radiation inside the material is assumed to consist of two isotropic diffuse fluxes propagating in opposite directions. The forward flux is termed $I(x)$, while the backward is termed $J(x)$.

The relations for the diffuse reflectance $R(\lambda)$ and transmittance $T(\lambda)$ for the material, that can be derived from the KM theory, describes the optical properties of the turbid material by an effective scattering coefficient S and an effective absorption coefficient K and the material thickness.

The coefficient K determines the attenuation of the diffuse light flux due to absorption, whereas S describes the net scattering of the flux between the forward ($I(x)$) and backward ($J(x)$) directions. The basic differential equations are given in Eq. (1) and (2).

$$-\frac{dI}{dx} = -(K + S)I(x) + SJ(x) \quad (1)$$

$$\frac{dJ}{dx} = -(K + S)J(x) + SI(x) \quad (2)$$

The following relationship between the ratio between K and S and the reflectance $R(\lambda)_\infty$ of a material with infinite thickness can be derived (Kortüm 1969),

$$\frac{K}{S} = \frac{(1 - R(\lambda)_\infty)^2}{2R(\lambda)_\infty} \equiv F(R_\infty) \quad (3)$$

where $F(R_\infty)$ is called the Kubelka-Munk function. When Eq. (3) is applied to a sample with finite thickness (d) the reflectance $R(\lambda)_d$ is typically approximated by the reflectance measured on a stack of the samples in question. Eq. (3) may be rewritten as,

$$\frac{K}{S} = \frac{(1 + R(\lambda))^2 - T(\lambda)^2}{2R(\lambda)} \quad (4)$$

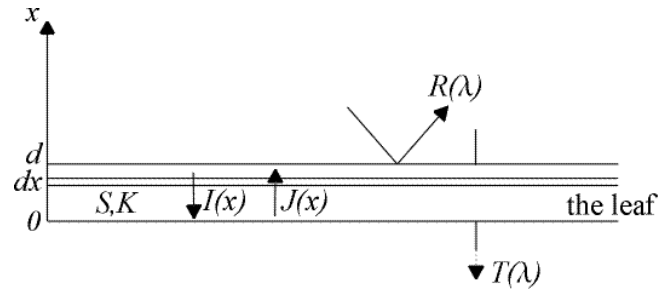


Fig. 5 The nomenclature used in the KM theory is shown in this figure for a single layer, which in this case is a leaf.

The R/T-EMP methods

The R/T-EMP methods are based on either the reflectance or transmittance values obtained at selected wavelengths and an empirical relationship between the reflectance or transmittance and the Chl concentration, which is determined by considering a statistically large number of plant material, including a variety of plants species. A discussion of some R/T-EMP methods can be found in (Cordón and Lagorio 2007) together with a discussion of the different correction methods that can be used to account for light re-absorption processes in leaves. The R/T-EMP method we have used in the calculation of the Chl concentration is the one derived in Gitelson *et al.* (2009). According to Gitelson *et al.* (2009) the Chl concentration in the unit nmol/cm^2 can be calculated as follows,

$$C_{chl} = (((R(\lambda))^{-1} - [R_{NIR}]^{-1}) - 0.001)/0.0018 \quad (5)$$

where $[R_{NIR}]$ is the average reflectance in the NIR spectral region and where it has been assumed that the Chl found in the leaves is mainly of the type a and b, hence the molar weight is $M = 1801 \text{ g/mol}$. Eq. (5) may be rewritten to give the Chl concentration in the unit $\mu\text{g}/\text{cm}^2$,

$$C_{chl} = 10^3 \cdot ((R(\lambda))^{-1} - [R_{NIR}]^{-1}) - 1 \quad (6)$$

Eq. (5) and (6) are found to be valid for reflectance values in the following spectral regions, 525 to 555 nm and 695 to 735 nm of the reflectance spectra. The average reflectance $[R_{NIR}]$ is used to correct the data for differences in the leaf thickness and structure. Specifically the average of the reflectance values in the wavelength region 750 nm to 800 nm has been used i.e. $[R_{NIR}]^{-1} = [R_{750}, R_{800}]^{-1}$. In the calculations presented in Tables 1 and 2 the Chl concentrations have been calculated as the averages of the values obtained from Eq. (5) with $\lambda = 550 \text{ nm}$ and 700 nm . In the case of leaves with similar properties as the leaves used to define Eq. (5) and (6) the accuracy of the Chl concentration can be estimated from Gitelson *et al.* (2009). The result is: $\pm 7 \mu\text{g}/\text{cm}^2$. Notice, however, that in cases, where the part of the plant considered behaves optically different, the uncertainty of the Chl concentration may be arbitrary.

Table 1 In the table are shown the calculated chlorophyll concentrations, in $\mu\text{g}/\text{cm}^2$, of the leaves from *Hibiscus* and *Chrysanthemum* using the two discussed models and the destructive method. The root mean square error (RMSE) of both methods is $\pm 7 \mu\text{g}/\text{cm}^2$ (Yamada and Fujimura 1991; Gitelson *et al.* 2003). The estimated uncertainty of the destructive method is $\pm 6\%$ (Arnon 1949).

Species	RT-MOD	R/T-EMP	Destructive
<i>Hibiscus</i>	43	72	-
<i>Chrysanthemum</i>	53	52	44

Table 2 The chlorophyll concentrations in $\mu\text{g}/\text{cm}^2$ of *Hibiscus* sepals and bracts are calculated from the reflectance and transmittance spectra.

Leaf type	RT-MOD	R/T-EMP
<i>Hibiscus</i> sepals, $U_1 = 0, V_1 = 0$	15	15
<i>Hibiscus</i> sepals, $V_1 \neq 0$	13	15
<i>Hibiscus</i> bracts, $U_1 = 0, V_1 = 0$	35	42
<i>Hibiscus</i> bracts, $V_1 \neq 0$	41	42

The empirical relation between the Chl concentration and inverse reflectance given in Eq. (6) may partially be explained in terms of the KM theory discussed in the preceding section.

First the leaf is considered as a single layer, which may be characterized by the phenomenological absorption and scattering coefficients K and S . When Eq. (4) is applied to the leaf, both the leaf and the background material contribute to the measured reflectance. In order to obtain the reflectance from the leaf alone, $R(\lambda)$, the reflectance is measured with the leaf placed in front of an ideal black, non-reflecting background or by having a light trap placed behind the leaf as is the case for the integrating sphere used in this paper. As seen in **Fig. 1** a chamber with a non-reflecting coating on the inner walls is placed behind the port P_1 .

In Gitelson *et al.* (2003) the nominator in Eq. (4), $(1 + R(\lambda)^2 - T(\lambda)^2)$, was plotted against the Chl concentration, determined by chemical methods, for a very large statistical material, including different types of plants i.e. maple, chestnut, wild vine and beech leaves. It was found that $(1 + R(\lambda)^2 - T(\lambda)^2)$ is approximately equal to 1 in the following spectral regions, 525 to 555 nm and 695 to 735 nm in cases, where $0 < R(\lambda) < 50$. It then follows from Eq. (4) that the ratio between the phenomenological absorption and scattering coefficients for the leaf becomes proportional to the reciprocal reflectance. In order to relate this result to the empirical relation in Eq. (6), the ratio between K and S must be proportional to the Chl concentration. This indicates that the scattering and absorption processes in the leaf must have different origins. It follows from the results obtained in Gitelson *et al.* (2003) that it is possible to correct for differences in the leaf thickness and structure by incorporating the reflectance from the near-infrared region, i.e. $[R_{750}, R_{800}]^{-1}$, into the model.

The RT-MOD methods

The RT-MOD methods are based on selected reflectance and transmittance values combined with a theoretical modeling of a leaf. Various models, which in a more or less complex way models biological processes and chemical content in leaves, have been developed (Yamada and Fujimura 1991; Jacquemoud and Ustin 2001). These models enable a non-destructive estimation of both Chl, carotenoid and anthocyanin concentrations. The different models are based on compromises between incorporating the leaf structure to a high degree of accuracy with a lot of parameters as a consequence and modeling the structure with only a few variables and the following faster method, which, however, may suffer from a lower degree of accuracy.

The RT-MOD used in the present paper is based on a model developed by Yamada and Fujimura (1991). In this model a leaf is considered a multilayered object, where each layer is approximated by a turbid medium, in which the absorption and scattering of light is described within the KM theory, discussed above.

The model therefore comprises two parts; the first part models the scattering and absorption of the single layers of the leaf, whereas the other part models the interaction between the layers, each characterized by different optical properties. Matrix calculations have been used to relate the model parameters of the different layers to the four quantities that can be obtained by experiment, namely the reflectance and transmittance measured by illuminating adaxial and abaxial sides of the leaf, respectively (Cordón and Lagorio 2007). The reflectance and transmittance measured, when the adaxial side is illuminated, are termed $R_a(\lambda)$ and $T_a(\lambda)$, respectively, while those referring to the abaxial side of the leaf are called $R_b(\lambda)$ and $T_b(\lambda)$, respectively. In order to reduce the number of parameters some simplifying assumptions for the different layers are invoked (see below) and finally the Chl concentration in the leaf is calculated by solving the matrix equations numerically. In the following a brief discussion is given together with the different assumptions that have been made with respect to the absorption and scattering properties of the tissues. A more thorough description can be found in (Yamada and Fujimura 1991).

The basic differential equations, which are similar to Eq. (1) and (2) but now valid for a single layer k of a leaf, are as follows,

$$-\frac{dI_k}{dx} = -(v_k + u_k)I_k(x) + u_k J_k(x) \quad (7)$$

$$\frac{dJ_k}{dx} = -(v_k + u_k)J_k(x) + u_k I_k(x) \quad (8)$$

where v_k and u_k denote the phenomenological absorption and scattering coefficients related to the Chl molecules present in the layer k , respectively, with the notation adopted from (Yamada and Fujimura 1991). Eq. (7) and (8) may be solved in terms of the reflectance and transmittance coefficients, r_k and t_k . When assuming that the Chl molecules in each volume element of the leaf absorb and scatter the light independently, then the Chl concentration becomes proportional to α_k and σ_k , which are the absorption and scattering cross sections associated with the Chl molecule bound in the particular tissue. Notice, that these cross sections are principally different from the cross sections for the free molecule discussed previously. If the Chl concentration m_k is calculated in $\mu\text{g}/\text{cm}^3$, then v_k and u_k can be expressed as

$$v_k = m_k \cdot \alpha_k \quad (9)$$

$$u_k = m_k \cdot \sigma_k \quad (10)$$

where α_k and σ_k are the scattering cross sections in $\text{cm}^2/\mu\text{g}$. It is convenient to introduce the dimensionless phenomenological absorption and scattering coefficients $V_k = v_k \cdot d_k$ and $U_k = u_k \cdot d_k$, where d_k is the thickness of the layer, which means that the Chl concentration M_k is now given in $\mu\text{g}/\text{cm}^2$. Eq. (9) and (10) are replaced by

$$V_k = \eta_k \cdot M_k \cdot \alpha_k + V_{0,k} \quad (11)$$

$$U_k = \eta_k \cdot M_k \cdot \sigma_k + U_{0,k} \quad (12)$$

where the absorption and scattering coefficients $V_{0,k}$ and $U_{0,k}$ account for the absorption and scattering from other molecular species in the layer k . The factor η_k describes the degree of collimation of the scattered light, where the subscript 1 indicates perfectly diffuse light and 1/2 collimated light. The differential equations, Eq. (7) and (8), may be expressed in terms of the dimensionless absorption and scattering coefficients, and the equations may be solved according to KM with respect to r_k and t_k .

Since, as already mentioned, the leaf is modeled with more layers, a system of coupled equations similar to Eq. (7) to (12) is obtained. When the Chl concentration and the optical parameters introduced above are known, the system of coupled equations can be solved numerically with respect to $R_a(\lambda)$, $T_a(\lambda)$, $R_b(\lambda)$ and $T_b(\lambda)$. Unfortunately, the coupled equations must be solved in reverse order, since it is the Chl concentration that is sought, which is more complicated. The complexity of the problem depends on the number and type of layers considered. **Fig. 6** shows the cross section of a leaf and illustrates the modeling and relevant parameters of a typical leaf with six layers.

The input to the model is the reflectance and transmittance values $R_a(\lambda)$, $T_a(\lambda)$ and $R_b(\lambda)$, $T_b(\lambda)$ obtained in three narrow (< 1 nm) bands at $\lambda_0 = 880$ nm, $\lambda_1 = 720$ nm and $\lambda_2 = 700$ nm. The band at $\lambda_0 = 880$ nm is chosen in a region, where only scattering is present. The choice of the bands at λ_1 and λ_2 has the effect that only scattering and absorption from Chl are accounted for in the calculations and hence the possible presence of scattering and absorption from other pigments is taken into account; see Eq. (8) and Eq. (10).

The novel idea of this model is that it can be used on leaves from different species, which is expected to contain different pigment compositions and concentrations.

When performing the actual calculation of the Chl concentration, a distinction must be made between the type of leaves, as they may differ with respect to the number and type of layers and the morphology/composition of the individual layers of tissue. The modeling of the interaction with light depends on the morphology and composition of the individual layers and the interaction between these. The model must therefore reflect if a layer is very dense due to a high number of highly packed chloroplasts, if the layer has a high concentration of one or multiple pigments or whether the layer contains only a limited number of scattered chloroplasts with a low concentration of pigments, such as the petals. A layer containing a high concentration of pigments has the same

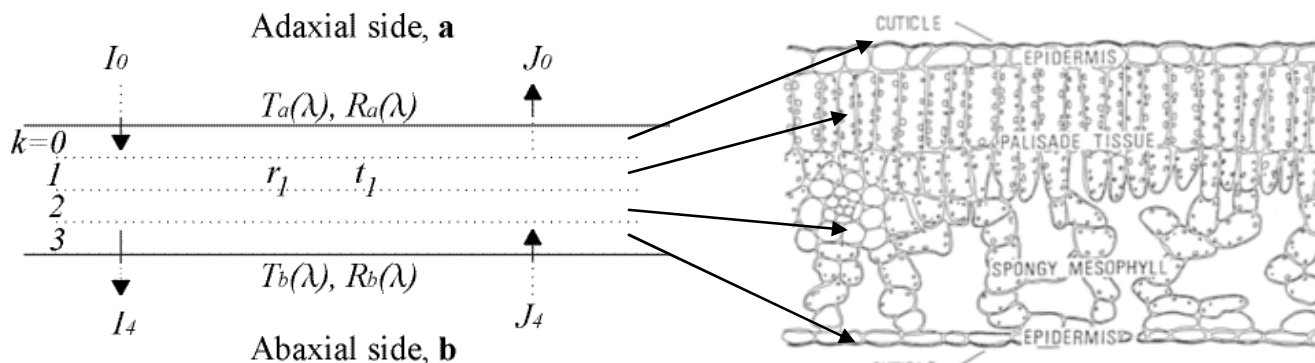


Fig. 6 The figure shows the cross section of a leaf, which is shown with permission from The Optical Society of America, and illustrates the modeling and relevant parameters of a typical leaf with six layers, besides, the nomenclature used in the KM theory is shown in this figure. When applying suitable knowledge about the optical characteristics of each tissue layer, this results in an optical/mathematical model of the leaf consisting of four layers.

effect as a dense layer, optically seen, that is, it results in a low penetration depth of the light. A tissue layer containing only highly scattered organelles (thus potentially a low concentration of pigments) will result in a high degree of scattering of the light. The type of scattering caused by the tissue depends on the size of the scattering organelles compared to the wavelength of the light.

Leaves are as a rule of thumb composed of up to six layers, i.e. the cuticula, epidermis, palisade and spongy mesophyll, epidermis and cuticula. The palisade layer may, however, consist of two or more layers depending on the species, or reflect differences in shade adaptation. For simplicity, the epidermis, which does not contain Chl, have been considered a part of the palisade and spongy mesophyll layer, respectively (Yamada and Fujimura 1991). That leaves the following layers to be incorporated into the model of a leaf:

- Layer no. 0, upper cuticula
- Layer no. 1, palisade mesophyll
- Layer no. 2, spongy mesophyll
- Layer no. 3, lower cuticula

Furthermore the upper and lower cuticula do not contain any pigments and hence do not exhibit any absorption. Thus, the sum of the reflectance and transmittance coefficients equals one for these tissues. The above numbering, i.e. 0 - 3, of the different type of tissues will be used, when specifying the different tissue parameters of the model.

The sepals and bracts from *Hibiscus* are considered to be composed of only three layers, i.e. the cuticula, epidermis, mesophyll, epidermis and cuticula. This means that when considering the modeling of the leaf, the sepals and bracts are composed of only three layers, namely the following:

- Layer no. 0, upper cuticula
- Layer no. 1, mesophyll
- Layer no. 2, lower cuticula

The modeling of the leaves follows hereafter, where the nomenclature used in Yamada and Fujimura (1991) has, for the most important parameters relevant for this short introduction, been given below.

- $r_0 = r_3 = 0.05$ and $t_0 = t_3 = 0.95$, where r_0 , t_0 and r_3 , t_3 are the reflectance and transmittance from the upper and lower cuticular tissue, respectively.
- It is used in the calculations that $U_1 = 0$, since the palisade tissue is densely packed and $V(\lambda_0) = 0$ since no absorption occurs at this wavelength.
- η describes the degree of collimation of the scattered light, where the subscript 1 indicates perfectly diffuse light and 1/2 collimated light. It is used in the calculations that $\eta_1 = 1/2$, $\eta_2(\lambda_0) = 1$
- the Chl concentration for the leaf M is given in the unit $\mu\text{g}/\text{cm}^2$, the relation between this concentration and the concentrations for each layer m_k is the probability P of finding Chl molecules in each layer

The model has been implemented in MatLab with the above assumptions, which are based on knowledge about the optical properties of the different leaves. This program can be required by contacting the corresponding author.

RESULTS AND DISCUSSION

The reflectance and transmittance spectra have been obtained from a leaf (**Fig. 7**), a sepal (**Fig. 8**) and a bract (**Fig. 9**) from a *Hibiscus rosa-sinensis* and from a leaf from *Chrysanthemum* (**Fig. 7**). These are the spectra used in the prediction of the Chl concentration, when using the optical model (Yamada and Fujimura 1991). The transmission measurements from each side of a leaf should be identical if this is not the case the average transmission values are used. **Figs. 4-7** contain the transmittance measurements, where both the raw data and the corrected values are shown. It is, besides, inherent for the optical model, that for the wavelength characterized by no absorption, the reflectance values from each side of the leaf should be identical. If this is not the case, the values should be scaled or corrected in order to achieve this (Yamada and Fujimura 1991). The upward facing side of the leaf is termed the **a**-side and the other side the **b**-side. With respect to the sepals, the side facing away from the bud is termed **a** and the other **b**. When the Chl concentration is predicted using the semi-empirical method (Gitelson *et al.* 2003), only the reflectance spectra are used, these are shown with the appropriate wavelengths marked (**Figs. 8, 9**). For the *Chrysanthemum* the results obtained by using the two methods have been compared to the Chl concentration estimated destructively as well. In this case the Chl extraction has been carried out as described by Arnon (1949) under cold and dark conditions. The concentration has been calculated by using a standard method as described in Arnon (1949). When calculating the Chl concentrations, Eq. (9) has been used for all *Hibiscus* leaves and Eq. (10) has been used for *Chrysanthemum*. Comparing the two types of leaves the appearances are very different, the *Chrysanthemum* being hairy and fragile and the *Hibiscus* strong and leathery. The Chl concentrations of the *Chrysanthemum* leaf (**Table 1**) show good agreement between the two methods, i.e. the optical model and the semi-empirical method (**Fig. 10**). The Chl concentration determined destructively is lower, but within the uncertainty of the methods.

To recap, the calculation of the Chl concentration using the R/T-EMP model, which is based on an empirical relationship between reciprocal reflectance and Chl concentration, has been calculated as the averages of the values obtained from Eq. (1) with $\lambda = 550$ nm and 700 nm for each type of leaf, i.e. leaf, bract and sepal. The calculation of the Chl concentration of these leaves using the RT-MOD, which is based on KM and the optical characteristics of the leaf, has been programmed in MatLab.

Based on these calculations it is found that the sepals contain a significantly lower concentration of Chl compared to the bracts and leaves, which contain approximately the same amount of Chl. The Chl concentrations calculated for the leaves of *Chrysanthemum* and *Hibiscus* show that the optical method yields consistent results, whereas it is likely

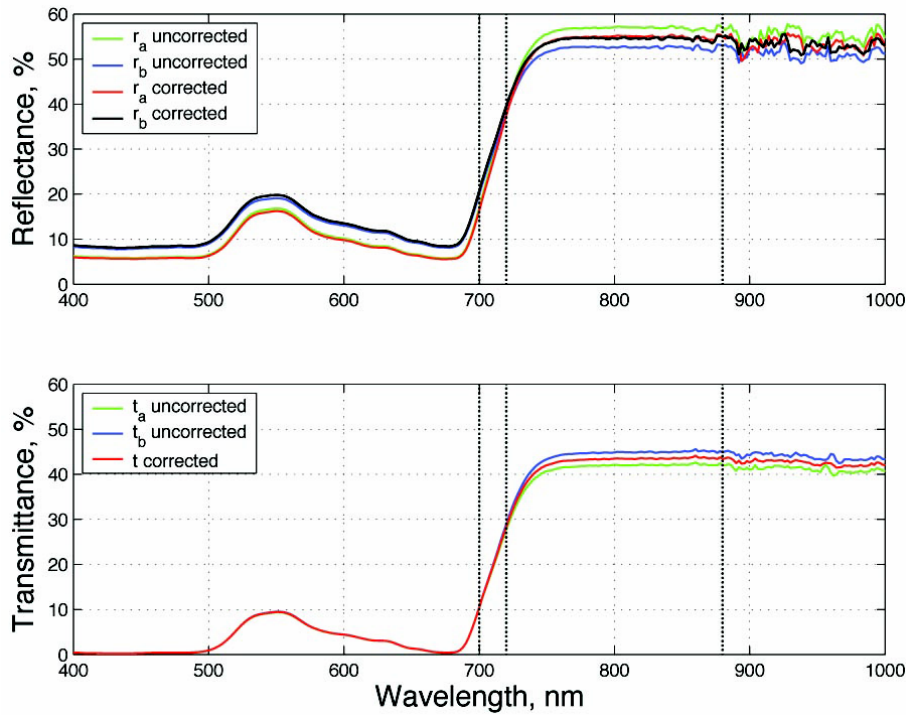


Fig. 7 Reflectance and transmittance spectra from the leaves of *Hibiscus*. The wavelengths $\lambda_0 = 880$ nm, $\lambda_1 = 720$ nm and $\lambda_2 = 700$ nm are marked, at which the reflectance/transmittance values are used in the calculation of the Chl concentration with the RT-MOD method. Corrected and uncorrected values are shown.

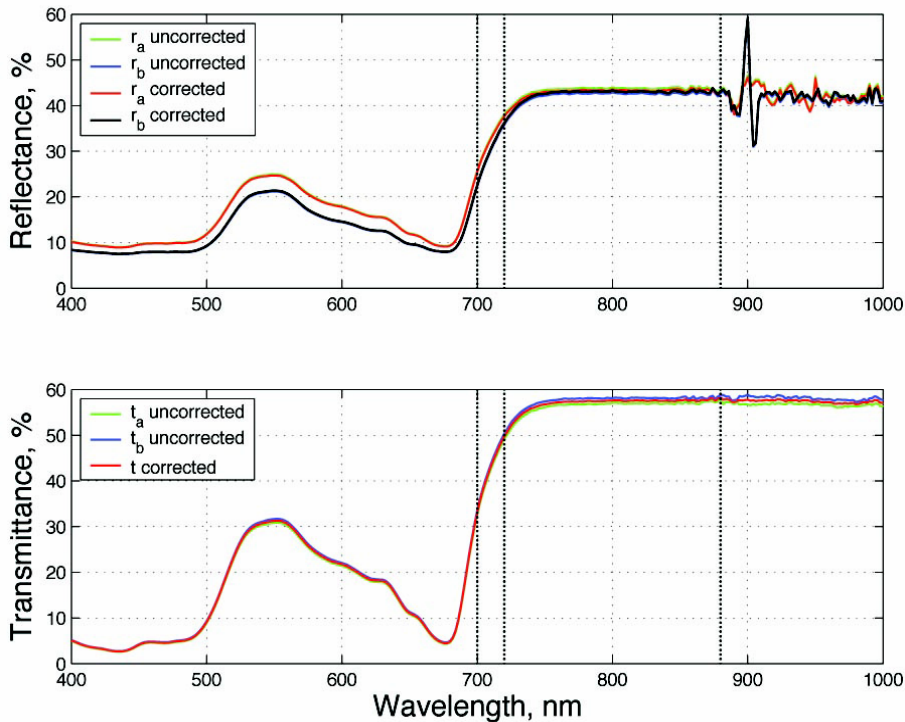


Fig. 8 Reflectance and transmittance spectra from the sepals of *Hibiscus*. The wavelengths $\lambda_0 = 880$ nm, $\lambda_1 = 720$ nm and $\lambda_2 = 700$ nm are marked, at which the reflectance/transmittance values are used in the calculation of the Chl concentration with the RT-MOD method. Corrected and uncorrected values are shown.

that the *Hibiscus* leaf (**Fig. 11**) does not fall within the sample space given by the semi-empirical method. The model proposed by Yamada and Fujimura (1991) remains valid for sepals from *Hibiscus*, provided that the parameters accounting for absorption and scattering with respect to the missing tissue layer are set equal to zero. This means, that with respect to the sepals and bracts from *Hibiscus*, the following assumptions are used $U_1 = 0$, $V_1 = 0$ and $\eta_1 = 0$. With respect to the Chl concentration of the *Hibiscus* leaves, the optical method yields a result that is of the same order of magnitude as the *Chrysanthemum* leaf (**Fig. 12**), while

the result from the semi-empirical method is much higher and far beyond the limits defined by the RMSE of the two methods. It should be noted that one of the important aspects of making the optical model, was to make a model that captures the diversity in Chl concentration exhibited by the different plant species (Yamada and Fujimura 1991). One of the pioneers of the field of non-destructive determination of pigment concentrations, Gitelson *et al.* (2003), has as already discussed developed the semi-empirical method, which is based on a very large statistical material, but comment in the conclusion that the applicability to other

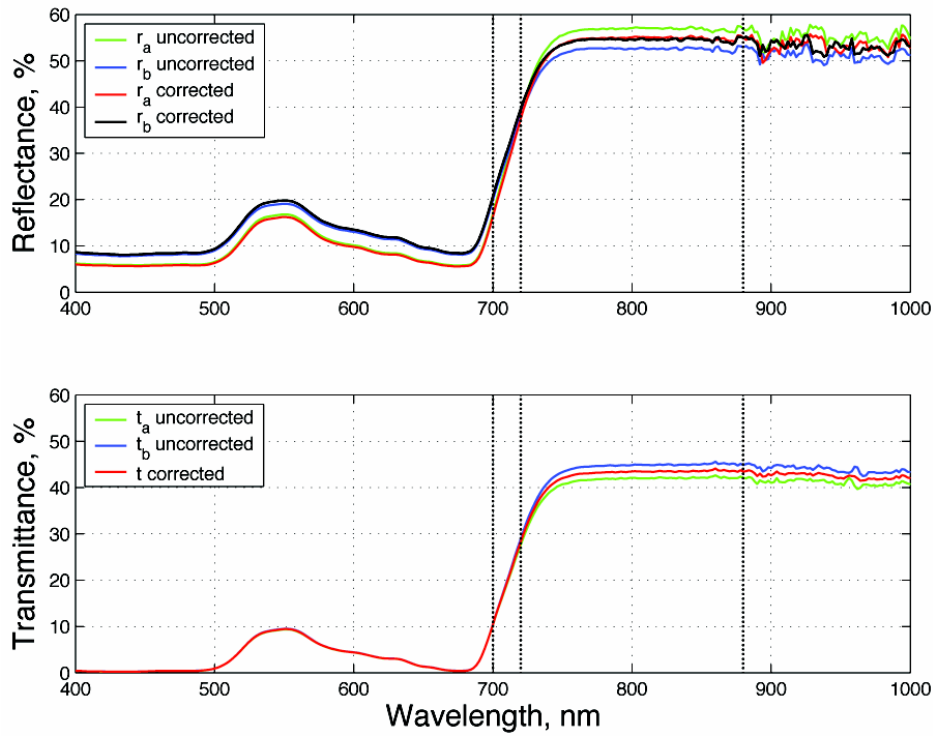


Fig. 9 Reflectance and transmittance spectra from the bracts of *Hibiscus*. The wavelengths $\lambda_0 = 880$ nm, $\lambda_1 = 720$ nm and $\lambda_2 = 700$ nm are marked, at which the reflectance/transmittance values are used in the calculation of the Chl concentration with the RT-MOD method. Corrected and uncorrected values are shown.

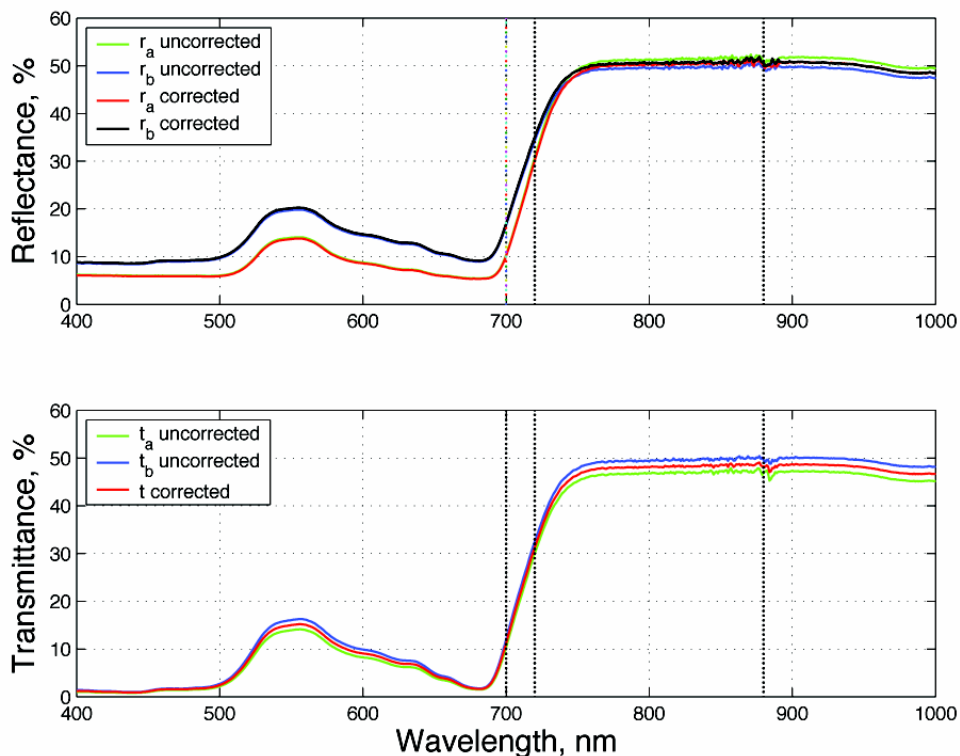


Fig. 10 Reflectance and transmittance spectra from the leaves of *Chrysanthemum*. The wavelengths $\lambda_0 = 880$ nm, $\lambda_1 = 720$ nm and $\lambda_2 = 700$ nm are marked, at which the reflectance/transmittance values are used in the calculation of the Chl concentration with the RT-MOD method. Corrected and uncorrected values are shown.

plant species, than the ones used, remains to be verified. In papers by Gitelson *et al.* (2003) and Gitelson and Merzlyak (2004), *Hibiscus* plants are part of the statistical basis, upon which the calculation of the Chl concentration is calculated for three different plant species. The concentration is, however, not calculated for *Hibiscus*, which could suggest deviating results. The conclusion seems to be that the *Hibiscus* leaf does not fit into the sample space given by the type of plants investigated in the semi-empirical method.

The values listed for the *Hibiscus* sepals and bracts in **Table 1** are calculated by using the earlier discussed assumption, namely that the sepals and bracts consist of only one tissue, which contain pigments, i.e. $U_1 = 0$ and $V_1 = 0$. For comparison purposes, the values obtained, if these leaves were considered to have a palisade tissue as well, are also calculated. This comparison gives an estimate of how sensitive the optical model is to such an assumption.

The results in **Table 2** show that the model and method

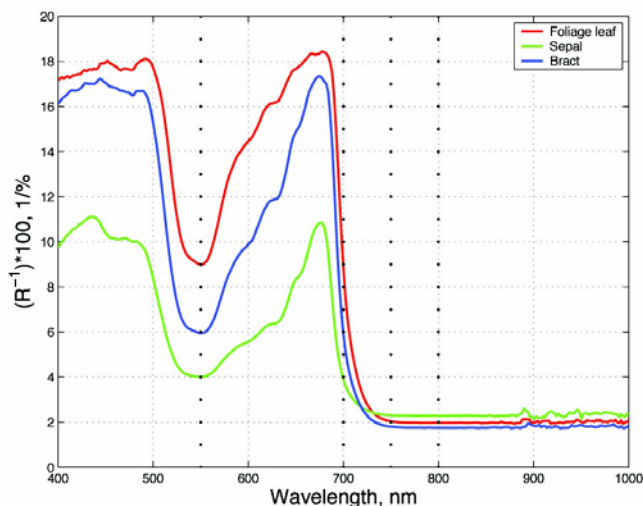


Fig. 11 The reciprocal reflectance of the leaves, sepals and bracts from *Hibiscus* with different wavelengths (550, 700, 750 and 800 nm) marked, at which the reflectance values are used in the calculation of the Chl concentration with the R/T-EMP method.

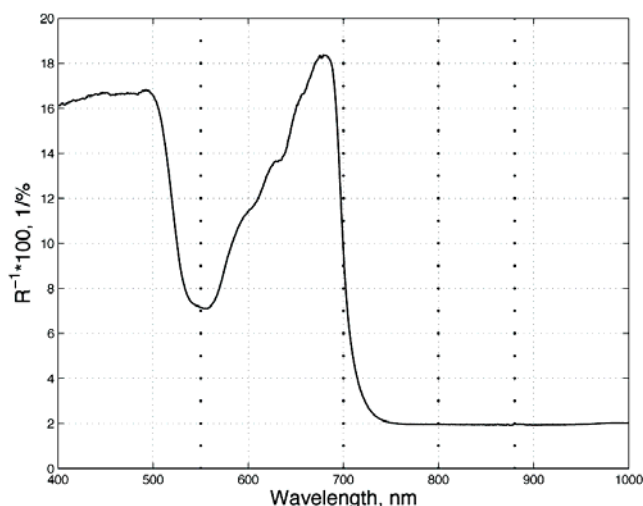


Fig. 12 The reciprocal reflectance of the leaves from *Chrysanthemum* with the different wavelengths (550, 700, 750 and 800 nm) marked, at which the reflectance values are used in the calculation of the Chl concentration with the R/T-EMP method.

render consistent results. The Chl concentration of the *Hibiscus* sepals calculated with the optical model together with the assumption that the leaf has got only one pigment containing tissue is consistent with the result obtained with the semi-empirical method, where the number of tissue layers is not a parameter.

A comparison of the results for the bract obtained from the optical and semi-empirical methods indicate that the bract has probably the same number of tissue layers as the leaf. It should be noted that the results obtained for one and two tissue layers are both within the estimated RMSE, which implies that further investigations are necessary in order to verify the exact number of tissue layers containing Chl. One way is to examine the cross sections by optical microscopy.

Note, that the measurements done in our previous paper showed that if the measurements were carried out with only a mask, the error would be of such dimensions that an estimation of the Chl concentration of the sepals and bracts would not have been possible (Jernshøj and Hassing 2009). In the long run, combinations of different methods with optimally chosen spectral bands might be used to estimate anthocyanin and Chl non-destructively and allow the deve-

lopment of handheld instrumentation enabling the estimation of pigment composition and concentration of fresh products (Merzlyak *et al.* 2002).

CONCLUDING REMARKS

We present a calculation of the Chl concentrations in different types of leaves from *Hibiscus rosa-sinensis* and *Chrysanthemum* based on non-destructive, optical measurements. We analyzed leaves, sepals and bracts from the *Hibiscus* and leaves from the *Chrysanthemum*, which represent samples from different species with a varying size.

Since the smaller sepals and bracts are too small to physically fit the aperture of the spectrophotometer, reproducible and accurate reflectance spectra of these leaves have been obtained by combining a mask with a properly focused sample beam, which has been adjusted so that no direct illumination of the mask takes place. The ratio between the mask aperture and the beam area has been chosen as large as the smallest samples allow, i.e. the bracts. With respect to the transmittance measurements a combination of a lens setup and an attachment of the sample to the entrance port have been used.

Two different models are used in the calculation of the Chl concentrations. The first model is based on an empirical relationship between reciprocal reflectance and Chl concentration. The second model incorporates the optical characteristics of the leaf structure into a mathematical model of the leaf.

The Chl concentrations calculated for the leaf of *Chrysanthemum* and *Hibiscus* show that the optical method gives consistent results, whereas it is believable that the *Hibiscus* leaf does not fall within the sample space defined by the semi-empirical method.

We have shown that the sepals contain a significantly lower concentration of Chl than both the bracts and the leaves and that the number of pigment containing tissue layers are assumed to be different in the sepals compared to the leaf and the bracts.

REFERENCES

- Arnon D (1949) Copper enzyme in isolated chloroplast polyphenoloxidase in *Beta vulgaris*. *Plant Physiology* **24**, 1-15
- Carter GA, Spiering BA (2002) Optical properties of intact leaves for estimating chlorophyll concentration. *Journal of Environmental Quality* **31**, 1424-1432
- Carter GA, Knapp AK (2001) Leaf optical properties in higher plants: Linking spectral characteristics to stress and chlorophyll concentration. *American Journal of Botany* **88**, 677-684
- Cordón GB, Lagorio MG (2007) Optical properties of the adaxial and abaxial faces of leaves. Chlorophyll fluorescence, absorption and scattering coefficients. *Photochemical Photobiological Science* **6**, 873-882
- Cordón GB, Lagorio MG (2006) Re-absorption of chlorophyll fluorescence in leaves revisited. A comparison of correction models. *Photochemical Photobiological Science* **6**, 873-882
- FieldScout CM 1000 Chlorophyll Meter Operation Manual, Catalog #2950, Spectrum Technologies, Inc., pp 1-28
- Fritsch F, Ray J (2007) Soybean leaf nitrogen, chlorophyll content, and chlorophyll a/b ratio. *Photosynthetica* **45**, 92-98
- Gitelson A, Chivkunova O, Merzlyak M (2009) Non-destructive estimation of anthocyanins and chlorophylls in anthocyanic leaves. *American Journal of Botany* **96**, 1861-1868
- Gitelson A, Gritz Y, Merzlyak M (2003) Relationships between leaf chlorophyll content and spectral reflectance and algorithms for non-destructive chlorophyll assessment in higher plant leaves. *Journal of Plant Physiology* **160**, 271-282
- Gitelson A, Merzlyak M (2004) Non-destructive assessment of chlorophyll, carotenoid and anthocyanin content in higher plant leaves: Principles and algorithms. In: Stamatiadis S, Lynch JM, Schepers JS (Eds) *Remote Sensing for Agriculture and the Environment*, Peripheral Editions 'ella', Larissa., Greece, pp 78-94
- Jacquemoud S, Ustin S (2001) Leaf optical properties: A state of the art. In: *8th International Symposium Physical Measurements and Signatures in Remote Sensing*, 8-12 January 2001, Aussois, France, CNES, pp 223-232
- Jernshøj K, Hassing S (2009) Analysis of reflectance and transmittance measurements on absorbing and scattering small samples using a modified integrating sphere setup. *Applied Spectroscopy* **63**, 879-888

- Kortüm G** (1969) *Reflectance Spectroscopy: Principles, Methods, Applications*, Springer Verlag, New York, 366 pp
- LabSphere PELA 1000** (Integrating sphere), Instruction Manual, AQ-01034-000 Rev.1, 1-39
- LabSphere PELA 1000** (Integrating sphere), A Guide to Reflectance Spectroscopy, Part No. 85-101222-000, pp 1-45
- Merzlyak M, Solovchenko A, Gitelson A** (2002) Reflectance spectral features and non-destructive estimation of chlorophyll, carotenoid and anthocyanin content in apple fruit. *Postharvest Biology and Technology* **27**, 197-211
- Murphy AB** (2006) Modified Kubelka-Munk model for calculation of the reflectance of coatings with optically-rough surfaces. *Journal of Physics: D: Applied Physics* **39**, 3571-3581
- Perkin Elmer, Lambda 900** (1996) Installation, Maintenance, System Description (0993-5037)
- Pflanz M, Zude M** (2008) Spectrophotometric analyses of chlorophyll and single carotenoids during fruit development of tomato (*Solanum lycopersicum* L.) by means of iterative multiple linear regression analysis. *Applied Optics* **47**, 5961-5970
- Smillie RM, Hetherington S** (1999) Photoabatement by anthocyanin shields photosynthetic systems from light stress. *Photosynthetica* **36**, 451-463
- SPAD 502 Plus Chlorophyll Meter** (2009) Product Manual Item # 2900P, 2900PDL, Spectrum Technologies, Inc., pp 1-24
- Yamada N, Fujimura S** (1991) Nondestructive measurement of chlorophyll pigment content in plant leaves from three-color reflectance and transmittance. *Applied Optics* **30**, 3964-3973
- Yang L, Miklavcic SJ** (2005) Revised Kubelka-Munk theory. III. A general theory of light propagation in scattering and absorptive media. *Journal of the Optical Society of America A* **22**, 1866-1873